Simulations of Ethylene Insertion in the Pt^{II}−H Bond of $(H)Pt(PX_3)_2^+$ Species

Betty B. Coussens,† Francesco Buda,‡ H. Oevering,† and Robert J. Meier*,†

DSM Research, P.O. Box 18, 6160 MD Geleen, The Netherlands, and INFM-FORUM, Scuola Normale Superiore, Piazza dei Cavalieri 7, I-56126 Pisa, Italy

Received February 3, 1997

Hartree−Fock, MP2, DFT, and Car−Parrinello type molecular dynamics simulations are reported applied to the insertion of ethylene in cationic platinum−hydrido−diphosphine complexes. The barrier to insertion is found to be small to negligible, which suggests that the insertion step itself is not rate-determining in a variety of catalytic processes including polymerization reactions, olefin isomerizations, hydroformylations, and hydrogenation reactions. The variation of the P−Pt−P bond angle throughout the reaction is found to be small, indicating that the complex can be relatively rigid while still allowing the insertion reaction to proceed. The energetics of the insertion reaction are hardly affected by electron-withdrawing or electron-donating groups on the phosphorus ligands (PH_3, PCl_3, PMe_3).

Introduction

The insertion of olefins into metal−hydrogen (M−H) bonds and the transformation of metal−alkyl compounds to olefins and metal hydrides by β-hydride elimination are important elementary steps in a variety of catalytic processes, such as polymerization reactions, olefin isomerizations, hydroformylations, and hydrogenation reactions.[1,2] For M = Pt, several experimental studies of the kinetics and mechanism of these elementary reaction steps have been published.[3−11] It is now generally accepted that the insertion of olefins into the Pt(II)−H bond of cationic platinum−hydride−phosphine compounds proceeds via a four-coordinated transition state having the phosphorus ligands in a cis position and the olefin parallel to the Pt−H bond (see Scheme 1).[8,12] Most experimental studies have focused on Pt(phosphine)$_2$ compounds where, due to the preferred trans coordination of the phosphine ligands, the trans−cis isomerization is a prerequisite for the insertion and elimination reactions to take place.[11] This isomerization step can be avoided by introducing a bridge between the phosphorus atoms that prevents trans coordination. Recently, the olefin insertion and elimination reaction for bridged Pt(bis-phosphine) compounds have been studied by Spencer and co-workers.[11−14] For [Pt(C$_2$H$_5$)(Bu$^t_2$P(CH$_2$)$_3$PBu$^t_2$)]$^+$, their NMR data appeared to be consistent with rapid intramolecular rearrangement processes involving both the ethylene−hydride form **1**, in which ethylene rotation is facile, and the alkyl form **2**, in which rotation of the methyl group is facile. They estimated the free energy of activation for these processes to be ca. 8 ± 1.5 kcal/mol, which serves as an upper bound for the energy difference between **1** and **2**. Furthermore, the Pt−alkyl form could be isolated. The X-ray crystal structure clearly indicated that this form was stabilized by the presence of a Pt−H$_\beta$ agostic interaction.

Scheme 1

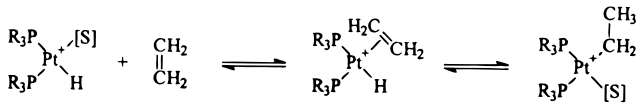

From a theoretical point of view, quite a number of studies have been reported over the past decade. A comprehensive survey was recently presented by Bray et al.[15] Several mechanistic alternatives for olefin insertion into the Pt(II)−H bond have been studied in detail by Thorn and Hoffmann[16] by means of extended Hückel calculations. It was found that the mechanism of Scheme 1 is indeed the most favorable one. To our knowledge, more advanced theoretical studies of the

* To whom correspondence should be addressed.
† DSM Research.
‡ INFM-FORUM, Scuola Normale Superiore.

(1) Collman, J. P.; Hegedus, L. S.; Norton, J. R.; Finke, R. C. *Principles and Applications of Organotransition Metal Chemistry*; University Science Books: Mill Valley, CA, 1987; Chapter 6.
(2) Yamamoto, A. *Organotransition Metal Chemistry*; Wiley: New York, 1986; Chapter 6.
(3) Chatt, J.; Shaw, B. L. *J. Chem. Soc.* **1962**, 5074−5084.
(4) McCarthy, T. J.; Nuzzo, R. G.; Whitesides, G. M. *J. Am. Chem. Soc.* **1981**, *103*, 1676−1678.
(5) Clark, H. C.; Jablonski, C. R.; Wong, C. S. *Inorg. Chem.* **1975**, *14*, 1332−1335.
(6) Brainard, R. L.; Whitesides, G. M. *Organometallics* **1985**, *4*, 1550−1557.
(7) Alibrandi, G.; Scolaro, L. M.; Minniti, D.; Romeo, R. *Inorg. Chem.* **1990**, *29*, 3467−3472.
(8) Romeo, R.; Alibrandi, G.; Scolaro, L. M. *Inorg. Chem.* **1993**, *32*, 4688−4694.
(9) Romeo, R.; Uguagliati, P.; Belluco, U. *J. Mol. Catal.* **1975/1976**, *1*, 325−366.
(10) Alibrandi, G.; Cusumanu, M.; Minniti, D.; Scolaro, L. M.; Romeo, R. *Inorg. Chem.* **1989**, *28*, 342−347.
(11) Carr, N.; Dunne, B. J.; Spencer, J. L. *J. Chem. Soc., Chem. Commun.* **1988**, 926−928.
(12) Mole, L.; Spencer, J. L.; Carr, N.; Orpen, A. G. *Organometallics* **1991**, *10*, 49−52.
(13) Carr, N.; Dunne, B. J.; Mole, L.; Orpen, A. G.; Spencer, J. L. *J. Chem. Soc., Dalton Trans.* **1991**, 863−871.
(14) Carr, N.; Mole, L.; Orpen, A. G.; Spencer, J. L. *J. Chem. Soc., Dalton Trans.* **1992**, 2653−2662.
(15) Bray, M. R.; Deeth, R. J.; Paget, V. J. *Prog. React. Kinet.* **1996**, *21*, 169−214.
(16) Thorn, D. L.; Hoffmann, R. *J. Am. Chem. Soc.* **1978**, *100*, 2079−2090.

S0276-7333(97)00080-0 CCC: $15.00
Publication on Web 02/04/1998

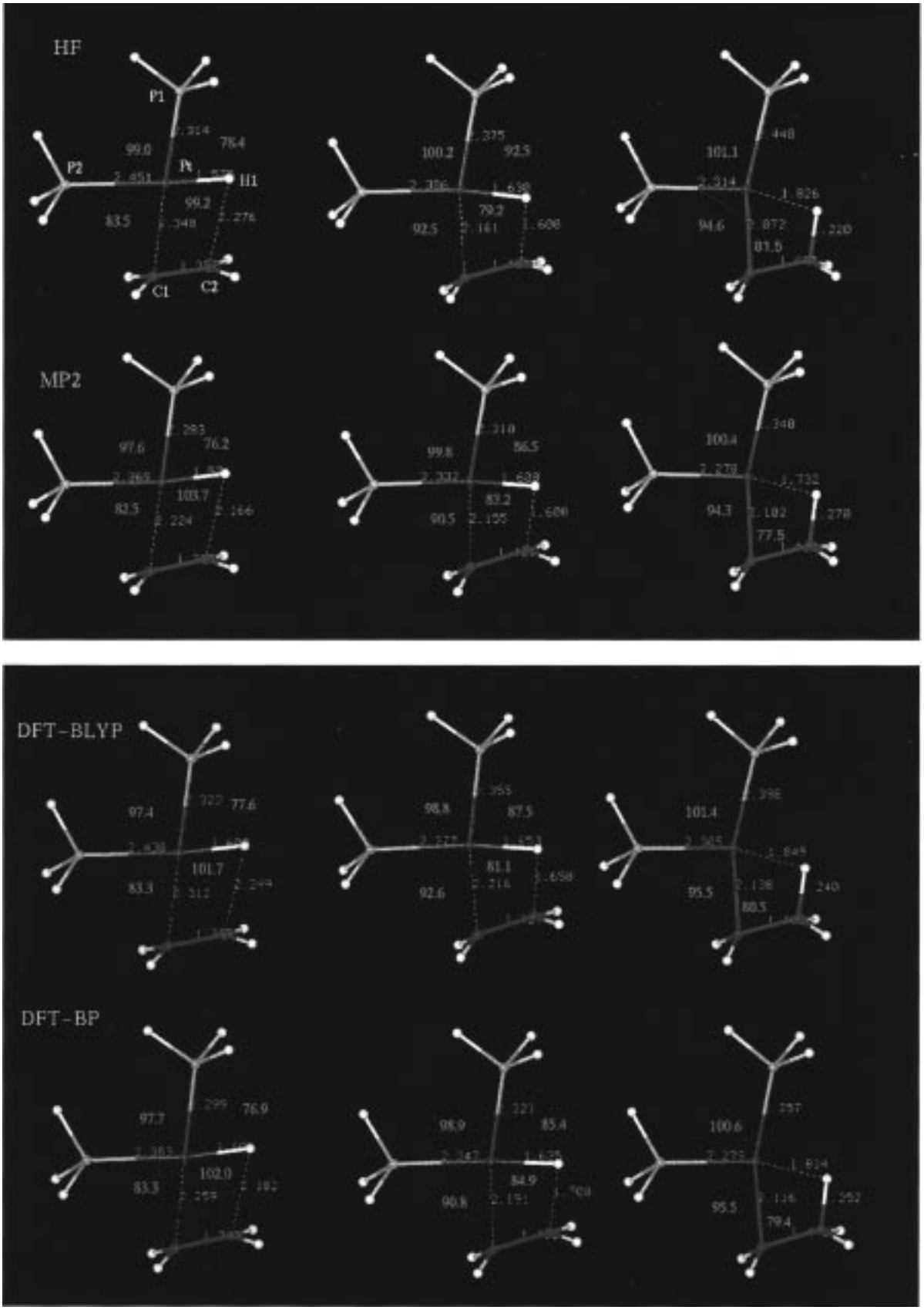

Figure 1. Optimized geometries for the reactant state, the transition state, and the product state for the $(H)Pt(PH_3)_2^+-C_2H_4$ system at the HF, MP2, DFT-BLYP, and DFT-BPW levels of theory.

insertion of olefin into the Pt(II)−H bond of Pt−phosphine compounds have only been performed for neutral species such as $(H)Pt(SiH_3)(PH_3)-(C_2H_4)$, investigated recently by Sakaki and co-workers.[17] In the current paper, we investigate the insertion of ethylene into the Pt(II)−H bond of $(H)Pt(PH_3)_2^+-C_2H_4$ using density functional, ab initio, and Car−Parrinello methods.

Table 1. Energetics of the Ethylene Insertion in the $(H)Pt(PH_3)_2^-(C_2H_4)^+$ System[a]

	HF	MP2	DFT-BLYP	DFT-BPW
reactant state (total energy)	0.0 (−882.133 528)	0.0 (−883.116 440)	0.0 (−884.790 460)	0.0 (−885.030 704)
transition state	4.4	2.6	2.7[b]	1.6[b]
β agostic product	1.3	1.1	0.1	−1.1
product state without agostic interaction	8.9	15.3	7.9	8.4

[a] Relative energies are in kcal/mol. Total energies (hartree) are for the (MP2-)HF optimized reactant structures. [b] At the DFT-BLYP level, the absolute value of the maximum component of the Cartesian gradient was 0.000 560, while at the DFT-BPW level it was 0.000 831.

The feasibility of studying chemical reactions using ab initio quantum molecular dynamics simulations employing the Car−Parrinello method[18] was first demonstrated in 1994.[19] Other recent studies involving this approach involved intramolecular hydrogen migration in $C_2H_2Li_2$,[20] the reaction of methane with $Rh(PH_3)_2Cl$,[21] and further investigations regarding ethylene insertion reactions in metallocenes.[22−24] In the present work we have therefore attempted to apply the Car−Parrinello method to study ethylene insertion in the Pt−H bond for the complexes $(H)Pt(PH_3)_2-C_2H_4$, $(H)Pt(PCl_3)_2-C_2H_4$, and $(H)Pt(PMe_3)_2-C_2H_4$.

Computational Details

Hartree−Fock, MP2, and DFT calculations were carried out by means of the Turbomole program,[25] version 2.30 for the MP2 calculations and version 950 for the DFT optimizations. In all of these calculations the core electrons of Pt (i.e., $1s^2-2s^22p^63s^23p^63d^{10}4s^24d^{10}4f^{14}$) were replaced by the relativistic effective core potentials of Ross et al.,[26] whereas the valence electrons were represented with a (5s5p4d)/[4s3p3d] basis set. Pure Hartree−Fock calculations including geometry optimization as well as single-point MP2//HF calculations were performed with DZP bases on all other atoms in the complex. In the single-point MP2//HF calculations the C1s, P1s, P2s, and P2p orbitals were frozen. In the MP2 and DFT optimization runs the same basis sets were employed, only with the exception of a DZ-quality basis set on the hydrogens of the PH_3 ligands. The DFT energies were calculated using the local VWN functional[27] including Becke's nonlocal exchange correction[28] and the Perdew[29] or Lee−Yang−Parr[30] nonlocal correlation correction.

For the computational details regarding the Car−Parrinello method type calculations we refer to refs 19 and 24. Vanderbilt type pseudopotentials were employed,[31] except for P, which involved a BHS type[32] pseudopotential. The Vanderbilt pseudopotential, including the scalar relativistic corrections according to the method outlined by Koelling and Harmon,[33] was used for Pt. An energy cutoff of 25 Ry was employed for the plane-wave expansion. The number of valence electrons selected for Pt was 18 and comprised $5s^25p^65d^96s^1$. Gradient corrections were included according to the schemes proposed by Perdew[29] and Becke.[34] The molecules treated had a dimension of 6−9 Å and were placed in a cubic box of 11.6 Å. When the van der Waals surface was drawn for each of the species, it could be clearly seen that they fit well within this box size, leaving some empty space. Energy minimization, using a steepest descent method (*largest* residual component of the gradient 0.008 hartree/bohr), was followed by a microcanonical (the total energy of the system is kept constant) MD simulation which was started at $T = 0$ K. If an exothermic chemical reaction takes place, the temperature of the system, evaluated from

$$T = (3Nk_B)^{-1}\sum_i^N {}^1/_2 m_i v_i^2$$

will increase. The initial velocities were chosen in the following way. Because no energy minimization procedure exerted on a molecule leads to *exactly* zero gradients, some residual gradients remain. During the first part of the dynamics simulations, the atomic velocities tend to develop along the directions of these residual gradients, as is likewise expected for a real system. This is particularly true for a barrierless situation, for which a residual gradient is directed along the reaction path.

Results and Discussion

1. HF, MP2, and DFT Calculations. The insertion process (Scheme 1) was investigated at the Hartree−Fock (HF) and MP2 levels by a stepwise variation of the distance between the hydrogen ligand (H1; cf. Figure 1 for the structure) and the nearest neighbor carbon atom of the ethylene (C2) from its value in the π-complex to its value in the product complex. For each constrained C2−H1 distance, all other degrees of freedom were completely relaxed. The relative energies of the reactant state, the transition state, and the product state corroborated from HF, MP2, and DFT calculations have been collected in Table 1. The corresponding structures have been presented in Figure 1. Since both the Hartree−Fock and the MP2 optimizations revealed the transition state at R(C2−H1) = 1.6 Å, in the DFT optimizations only the region with R(C2−H1) ranging from 1.5 to 1.7 Å was explored.

The HF activation energy was calculated to be 4.4 kcal/mol. In accordance with recent experience, see, e.g., Ahlrichs et al.,[35] the barrier is lowered by the inclusion of correlation effects. At the single-point MP2

(17) Sakaki, S.; Kato, H.; Kanai, H.; Tarama, K. *Bull. Chem. Soc. Jpn.* **1975**, *48*, 813−818.
(18) Car, R.; Parrinello, M. *Phys. Rev. Lett.* **1985**, *55*, 2471−2474.
(19) Meier, R. J.; Van Doremaele, G. H. J.; Iarlori, S.; Buda, F. *J. Am. Chem. Soc.* **1994**, *116*, 7274−7281.
(20) Röthlisberger, U.; Klein, M. L. *J. Am. Chem. Soc.* **1995**, *117*, 42−48.
(21) Margl, P.; Ziegler, T.; Blöchl, P. *J. Am. Chem. Soc.* **1995**, *117*, 12625−12634.
(22) Iarlori, S.; Buda, F.; Van Doremaele, G. H. J.; Meier, R. J. *Makromol. Chem., Macromol. Symp.* **1995**, *89*, 369−372.
(23) Van Doremaele, G. H. J.; Meier, R. J.; Iarlori, S.; Buda, F. *J. Mol. Struct. (THEOCHEM)* **1996**, *363*, 269−278.
(24) Iarlori, S.; Buda, F.; Meier, R. J.; Van Doremaele, G. H. J. *Mol. Phys.* **1996**, *87*, 801−815.
(25) Computational results were obtained using software programs from Biosym/MSI of San Diego; ab initio calculations were done with the Turbomole program, and graphical displays were printed out from the Insight molecular modeling system.
(26) Ross, R. B.; Powers, J. M.; Atashroo, T.; Ermler, W. C.; LaJohn, L. A.; Christiansen, P. A. *J. Chem. Phys.* **1990**, *93(9)*, 6654−6670.
(27) Vosko, S. H.; Wilk, L.; Nussair, M. *Can. J. Phys.* **1980**, *58*, 1200.
(28) Becke, A. D. *Phys. Rev. B* **1988**, *38*, 3098−3100.
(29) Perdew, J. P. *Phys. Rev. B* **1986**, *33*, 8822−8824.
(30) Lee, C.; Yang, W.; Parr, R. G. *Phys. Rev. B* **1988**, *37*, 785−789.
(31) Vanderbilt, D. *Phys. Rev. B* **1990**, *41*, 7892−7895.
(32) Bachelet, G. B.; Hamann, D. R.; Schlüter, M. *Phys. Rev. B* **1982**, *26*, 4199−4228.
(33) Koelling, D. D.; Harmon, B. N. *J. Phys. C (Solid State Phys.)* **1977**, *10*, 3107−3114.
(34) Becke, A. *J. Chem. Phys.* **1992**, 96, 2155−2160.
(35) Weiss, H.; Ehrig, M.; Ahlrichs, R. *J. Am. Chem. Soc.* **1994**, *116*, 4919−4928.

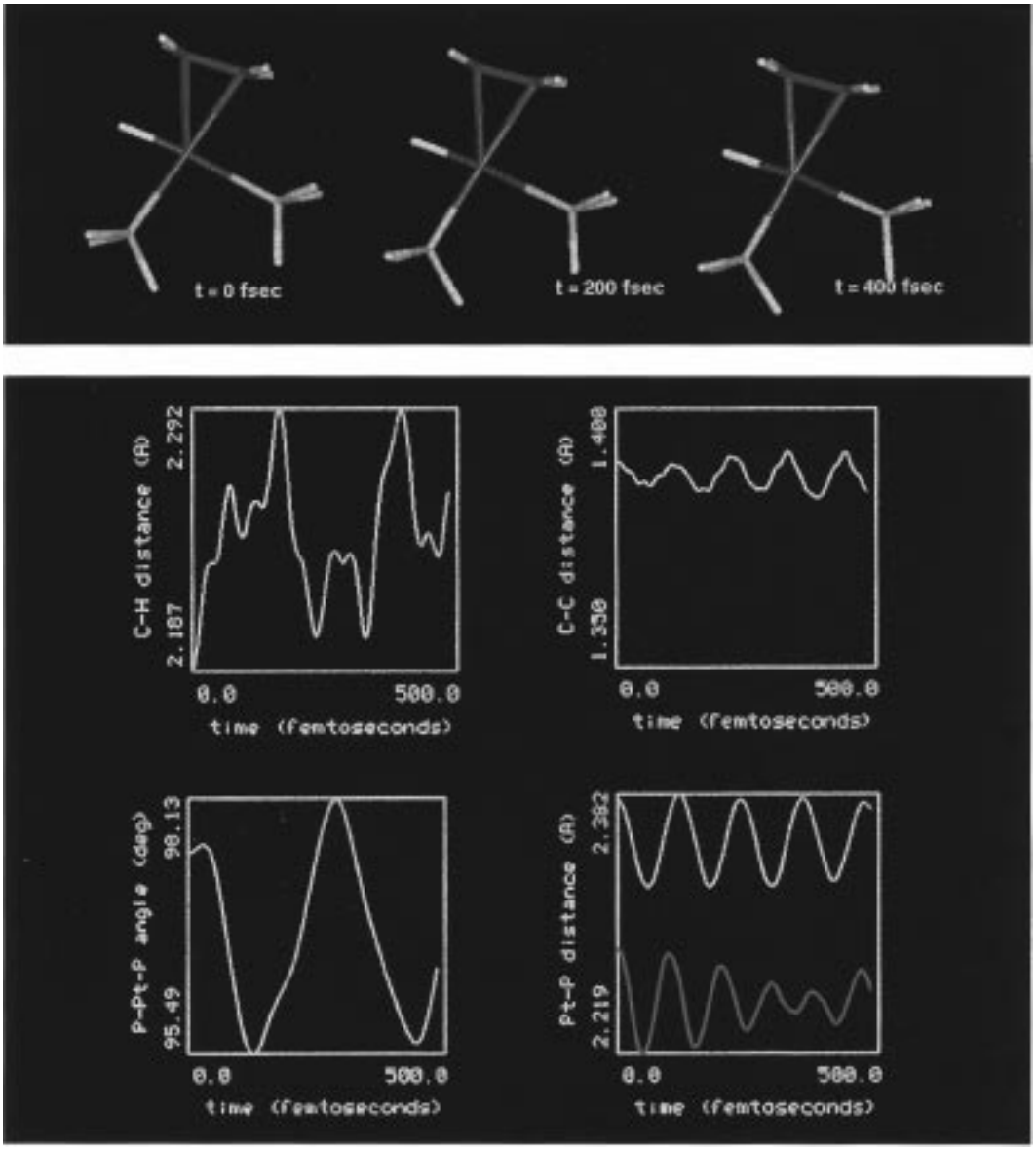

Figure 2. Time evolution of the (H)Pt(PH_3)$_2$−C_2H_4 complex during the molecular dynamics simulation. A few structures are shown, taken as snapshots along the dynamics trajectory, at the times (in femtoseconds) indicated with the structures. The graphs show the variation of some geometrical parameters during the dynamics simulation. The time evolution of the (Pt)H1−C1(ethylene) distance shows the absence of insertion of ethylene within the time span of the simulation. The next graph shows the ethylene C−C distance, followed by a graph displaying the variation of the P−Pt−P angle. The last graph shows the time variation of the Pt−P distances.

level the barrier decreases to 1.0 kcal/mol; at the MP2 optimized level a barrier of 2.6 kcal/mol was obtained, and the DFT calculations have revealed barriers of 2.7 kcal/mol (DFT-BLYP) and 1.6 kcal/mol (DFT-BPW), respectively. These results indicate that correlation effects are far less important in the study of the model reaction (H)Pt(PH_3)$_2$(C_2H_4) → Pt(PH_3)$_2$(C_2H_5)$^+$ than for the $Cp_2TiCH_3^+$−C_2H_4 system.[35] However, as was also observed for the case of ethylene insertion in various metallocenes,[19,22,23,35−39] the absolute magnitude of the barrier at the higher (correlated) levels of theory clearly suggests that this step is not rate-determining in the overall chemistry. Finally, the overall enthalpy of reaction was calculated to be close to zero (varying from −1.1 to +1.3 kcal/mol) at all levels of theory. Consequently, the reverse reaction involving β-hydrogen elimination is also facile (small barrier), in agreement with experimental data from Spencer et al.[11−14]

Regarding changes in the geometry of the complex along the reaction path, a significant change in the trans influence of the ligands was revealed. As the C2−H1 bond is formed, the Pt−H1 bond weakens, thereby reducing the trans influence of the hydride. During the ethylene insertion reaction the Pt−H1 distance becomes considerably longer while the Pt−P2 distance becomes shorter. The Pt−P1 bond, on the other hand, is significantly weakened (becoming longer) during the insertion reaction due to the formation of the Pt−C1 σ-bond. As

(36) Woo, T. K.; Fan, L.; Ziegler, T. *Organometallics* **1994**, *13*, 432−433.
(37) Woo, T. K.; Fan, L.; Ziegler, T. *Organometallics* **1994**, *13*, 2252−2261.
(38) Lohrenz, J. C. W.; Woo, T. K.; Fan, L.; Ziegler, T. *J. Organomet. Chem.* **1995**, *497*, 91−104.
(39) Lohrenz, J. C. W.; Woo, T. K.; Fan, L.; Ziegler, T. *J. Am. Chem. Soc.* **1995**, *117*, 12793−12800.

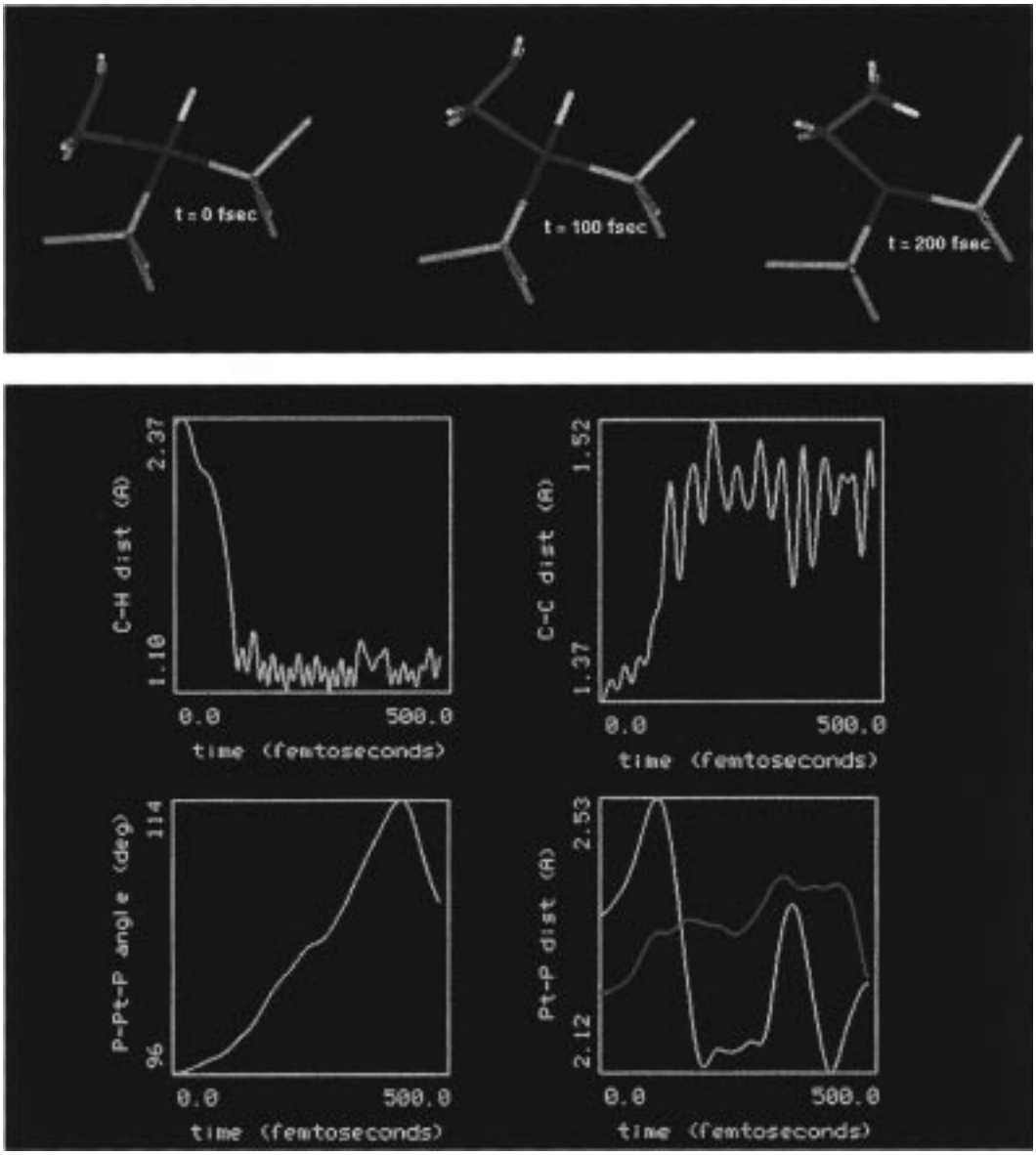

Figure 3. Variation of some geometrical parameters during the dynamics simulations of the $(H)Pt(PCl_3)_2-C_2H_4$ complex. The time evolution of the (Pt)H1−C1(ethylene) distance clearly reveals the completion of the insertion of ethylene. The next graph shows the ethylene C−C distance, which starts at the ethylene carbon−carbon double-bond distance and then starts developing toward a single bond with large bond length fluctuations. The third graph shows the variation of the P−Pt−P angle. For further discussion see the text. The last graph displays the time variation of the Pt−P distances, which shows a crossing indicating that the relative bond lengths interchange during the reaction, i.e., before and after the reaction.

one goes along the reaction path, the relative lengths of the Pt−P1 and Pt−P2 bonds are reversed, being almost equal at the transition state. At all four levels of calculation a very small variation in the P−Pt−P angle along the reaction path is observed. As can be seen from Figure 1, this angle varies from ca. 97° in the starting complex to ca. 100° in the transition state. This variation of only ca. 3° is significantly smaller than the change in the P−Pt−P angle as obtained from the extended Hückel calculations of Hoffmann and co-workers.[16] The latter revealed an optimum P−Pt−P angle of 95° in the reagent complex and 110° in the transition state.

As can be seen from the product structures displayed in Figure 1, the direct product of the insertion reaction is found to be characterized by an agostic $Pt-H_\beta$ interaction. The strength of the agostic interaction can be estimated by eliminating this interaction through a rotation of the ethyl group around the C−C bond. The resulting structure with the ethyl group in the internally staggered conformation was therefore optimized by imposing C_s symmetry (a symmetry plane through the plane containing all heavy atoms of the system (Pt, P1, P2, C1, C2) was imposed). The relative energy of the internally staggered structure with no agostic interaction, compared to the structure involving an agostic interaction, was calculated as 7.6 kcal/mol at the HF level, 14.2 kcal/mol at the MP2 optimized level, and 7.8 and 9.5 kcal/mol at the DFT-BLYP and DFT-BPW levels, respectively. In each case the structure with the agostic interaction was found to be the more stable structure. In agreement with the results of Sakaki and co-workers,[17] the agostic interaction is thus found to be considerably stronger at the MP2 than at the HF level.

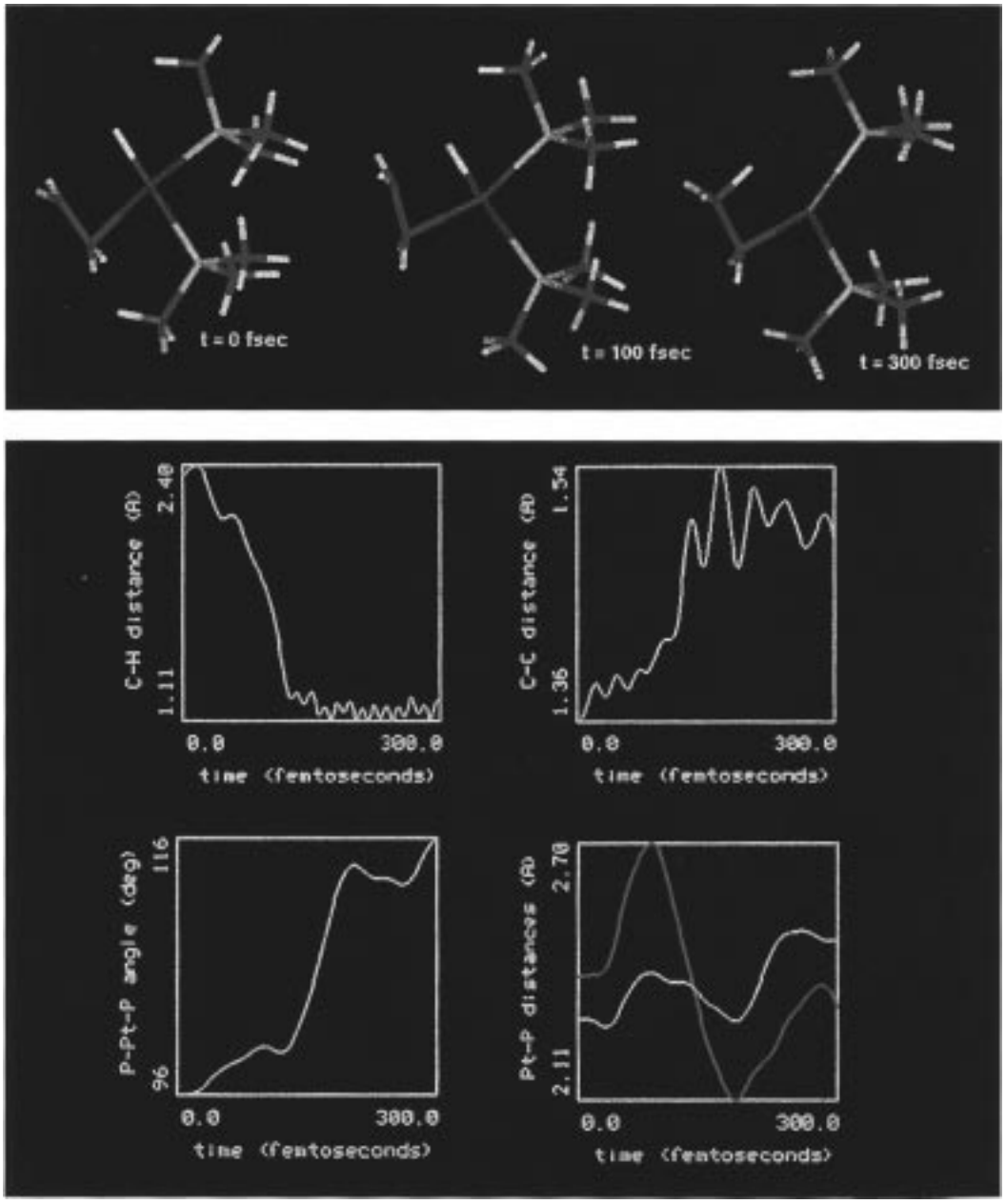

Figure 4. Variation of geometrical parameters during the dynamics simulations of the $(H)Pt(PMe_3)_2-C_2H_4$ complex. The time evolution of the (Pt)H1−C1(ethylene) distance clearly reveals the completion of the insertion of ethylene. The next graph shows the ethylene C−C distance, which starts at the ethylene carbon−carbon double-bond distance and then starts developing toward a single bond with large bond length fluctuations. The third graph shows the variation of the P−Pt−P angle. For further discussion see the text. The last graph displays the time variation of the Pt−P distances, which shows a crossing indicating that the relative bond lengths interchange during the reaction, i.e., before and after the reaction.

2. Ab Initio Molecular Dynamics (Car−Parrinello) Simulations. The geometry of the $(H)Pt(PH_3)_2-C_2H_4$ optimized complex is practically identical with the structure obtained by the DFT-BPW method implemented within the Turbomole package (see Figure 1 for the latter geometry). More specifically, Pt−H = 1.61 Å, P−Pt−P = 97.6°, and H−Pt−P = 77.0° obtained for the plane-wave-based optimization is to be compared with Pt−H = 1.61 Å, P−Pt−P = 97.7°, and H−Pt−P = 76.9° for the DFT-BPW calculation performed with a localized basis set (Turbomole). The effect of the relativistic corrections on the initial geometry is important, as its neglect led to the values Pt−H = 1.67 Å, P−Pt−P = 95°, and H−Pt−P = 85° using the plane-wave-based Car−Parrinello method.

Figure 2 shows the most important features corroborated from the simulations performed on $(H)Pt(PH_3)_2-C_2H_4$. Figures 3 and 4 show the corresponding information for $(H)Pt(PCl_3)_2-C_2H_4$ and $(H)Pt(PMe_3)_2-C_2H_4$, respectively. In Figures 2−4 graphs are shown displaying the distance between one of the ethylene carbon atoms and the single H bonded to the Pt. These two atoms are presumed to form a bond in the real, experimental reaction. As is apparent from these figures, our simulations did reveal the actual reaction for the species with the PCl_3 and the PMe_3 ligands, whereas the species with the PH_3 ligand did not show insertion within the time span of this simulation (a simulation in which the relativistic correction was omitted revealed direct insertion for the PH_3 species as

well). These results are in agreement with the MP2 and DFT results for the $(H)Pt(PH_3)_2-C_2H_4$ system presented above, which suggest a small barrier for this system.

The time scales for completion of the insertion for the species with PCl_3 and PMe_3, which are roughly 100 fs (see Figures 3 and 4), should not be confused with the true reaction rate. The real, experimental reaction takes place in solution. Consequently, the true rate is at least diffusion-limited and is possibly affected by the type of solvent. It has been common practice to neglect the latter in computer simulations, which is obviously not a justification, for reasons of feasibility of the simulations (there are first indications, however, that the Car−Parrinello MD method allows for such simulations to be practically carried out). In summary, the very short time scales which we found for ethylene insertion in several $Pt^{II}-H$ bonds do not have a realistic meaning as far as the overall reaction rate is concerned but indicate that the insertion step itself is not rate-determining.

Figures 2−4 show the variation, during the simulations, of various other geometrical parameters. For the PCl_3 and the PMe_3 cases, which show insertion during the simulation, the ethylene internal C−C bond is seen to lengthen quite abruptly near the moment of completion of the reaction (viz. the C−C plot), while fluctuations in this C−C bond length remain significant even after the insertion has completed. For the PH_3 complex the P−Pt−P bond angle does not vary significantly during this *dynamics* simulation, whereas in particular for the species with the PMe_3 ligands this angle continues to increase up until the end of the current simulation (see third graph in Figure 4). These data suggest that the P−Pt−P bond angle might open to a significant extent during the reaction. For the two systems which exhibit insertion, the relative lengths of the Pt−P distances interchange as one goes along the reaction path (fourth graph in Figures 3 and 4). In addition, for the two systems showing barrierless insertion, it is interesting to note that the dynamics simulations show that both Pt−P distances in each molecule fluctuate much more strongly than what is expected for a normal molecular vibration, i.e., as for the case of the PH_3 species.

Finally, we make a remark regarding the temperature during the simulation. Since we performed microcanonical simulations starting at $T = 0$ K, the temperature is expected to rise during simulation when an exothermic chemical reaction proceeds. When the rise in temperature is extreme, the observed behavior during the dynamics simulations might be unrealistic compared to room-temperature behavior. In the present simulations, the maximum temperature reached during each of the simulations was $T_{max} = 6$ K for PH_3, $T_{max} = 240$ K for PCl_3, and $T_{max} = 290$ K for PMe_3, from which we conclude that no exotic chemistry is expected to occur. The low rise in temperature for the PH_3 system is in agreement with the absence of a chemical reaction during the simulation presented here.

Final Discussion and Conclusions

Various ab initio type simulations have been performed on the insertion of ethylene in the $Pt^{II}-H$ bond of a number of $(H)Pt(PX_3)_2^+-C_2H_4$ systems. For X = H, simulations were carried out at the HF and the MP2 levels and DFT calculations using two different functionals were reported (DFT-BLYP and DFT-BPW). Furthermore, a quantum molecular dynamics study using the Car−Parrinello method was performed. The static simulations have revealed barriers to insertion of the ethylene which varied from 4.4 kcal/mol (HF), 2.6 kcal/mol (MP2), and 2.7 kcal/mol (DFT-BLYP) down to 1.6 kcal/mol (DFT-BPW). The (MP2/)HF results suggest a lowering of the barrier upon accounting for electron correlation (MP2). This is confirmed by the DFT results, which both yield values significantly lower than those for the pure HF level. The observation from the Car−Parrinello simulations that the insertion does not proceed instantaneously is in agreement with the (small) barrier found from the static DFT calculations.

The dynamics simulations on the platinum−phosphine complexes with X = Cl and X = Me showed very fast insertion of the ethylene. The small barrier calculated for the PH_3-containing complex and the fast insertion seen for the PCl_3 and PMe_3 systems suggests that the energetics of the insertion reaction are hardly affected by electron-withdrawing or electron-donating groups on the phosphorus ligands. Since the barriers are all relatively small, as revealed from either the static or the dynamic simulations, we think they are practically the same within the limits of accuracy of the levels of calculation employed.

The very short time scales (∼100 fs) which we found for ethylene insertion in the various $Pt^{II}-H$ bonds do not have a realistic meaning as far as the overall reaction rate is concerned but indicate that the insertion step itself is not rate-determining. Probably the most relevant conclusion from the present study is that, as for ethylene insertion in bis(cyclopentadienyl)metallocene species[19,22,23,35−39] and contrary to what was often the traditional point of view, this is another example of a reaction cycle for which the insertion step turns out not to be rate-determining.

Acknowledgment. We wish to acknowledge David Vanderbilt for providing the atomic code used to generate the relativistic pseudopotential for platinum. We thank the reviewers for making very useful comments on the first version of this paper. The management of DSM Research is acknowledged for their permission to publish this work.

OM970080O